

Performance of Polymer Electrolyte Membrane Fuel Cells Made from Sulfonated Polyimides

Otoo Yamada, Yan Yin*, Kazuhiro Tanaka*, Hidetoshi Kita*, Ken-ichi Okamoto*

Venture Business Laboratory, Yamaguchi University

* Department of Advanced Materials Science & Engineering, Faculty of Engineering, Yamaguchi University

2-16-1 Tokiwadai, Ube, Yamaguchi 755-8611, Japan

Fax: 81-836-85-9601, e-mail: oyamada@yamaguchi-u.ac.jp, okamoto@yamaguchi-u.ac.jp

Membrane electrode assemblies (MEAs) were made from two types of sulfonated polyimides (SPIs), namely, the linear and main-chain type SPI and the branched, crosslinked and side-chain type SPIs. Their single cell performance for H_2/O_2 was evaluated at a cell temperature of $70^\circ C$, humidifier temperatures of 70 and $68^\circ C$ for anode and cathode, respectively, and a total pressure of 0.3 MPa, and compared with that of Nafion 115 and 112. The MEAs made from the branched, crosslinked and side-chain type of SPIs showed the high performance, for example, a maximum output of 1.26 W/cm² at a current density of 3.7 A/cm², which was comparable or superior to that of Nafion 112 and much better than that of Nafion 115 and the linear and main-chain type of SPI. This was probably because of the thinner membrane with reasonably high proton conductivity and the better contact of membrane and electrode interface. Effects of operating conditions on cell performance were also investigated.

Key words: sulfonated polyimide, fuel cell, polymer electrolyte membrane, proton conductivity, membrane electrode assembly

1. INTRODUCTION

Polymer electrolyte membrane fuel cells (PEMFCs) have received great attention as power sources for vehicle, stationary cogeneration systems and portable electric instruments such as cellular phone and notebook type computer [1, 2]. In a PEMFC, the fuels, H_2 at the anode and O_2 at the cathode, are converted by an electrochemical reaction into H_2O , heat and electrical energy. Perfluorosulfonic acid electrolyte membranes, such as Nafion have the outstanding mechanical and chemical stability and high proton conductivity. However, they have some weak points such as high methanol permeability, lower operation temperature, high cost, and high fluorine content, which limit their further application.

Among the alternative proton exchange membranes investigated up to date, sulfonated polyimide (SPI) is one of the leading materials because of the reasonably high proton conductivity, good film-forming ability and relatively high durability under severe thermal and chemical conditions. Their synthesis and basic physical properties have been reported [3-10].

In this paper, we prepared MEAs composed of two Pt/C electrodes and SPI membrane and their single cell performance were evaluated for H_2/O_2 and H_2 /air systems and compared with that of Nafion 115.

2. EXPERIMENTAL

Two types of SPIs, namely the linear and main-chain type and the branched, crosslinked and side-chain type, were used in this study. Figure 1 shows their chemical structures. The linear and main-chain type of SPI is

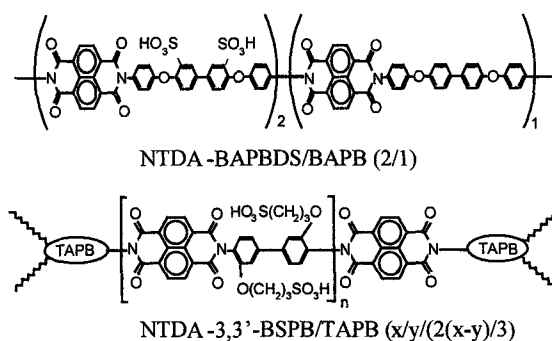


Fig.1 Chemical structures of SPIs.

NTDA-BAPBDS/BAPB(2/1), which was prepared by polycondensation of 1,4,5,8-naphthalenetetracarboxylic dianhydride (NTDA) with 4,4'-bis(4-amino-phenoxy)-biphenyl-3,3'-disulfonic acid (BAPBDS) and 4,4'-bis(4-aminophenoxy)biphenyl (BAPB) in a molar ratio of BAPBDS/BAPB of 2/1 [7,8]. The branched, crosslinked and side-chain type of SPI is NTDA-3,3'-BSPB/TAPB [$x/y/(2(x-y)/3)$], which was prepared by the following one-pot process. First, the anhydride-terminated oligomer of side-chain type SPI was prepared in *m*-cresol solution from NTDA and 3,3'-bis(3-sulfopropoxy)benzidine (3,3'-BSPB) in a molar ratio of NTDA/3,3'-BSPB of x/y [9,10]. Then, to the oligomer solution, a $2(x-y)/3$ portion of tris(4-aminophenoxy)-benzene (TAPB) was added with stirring and the solution was heated at $60-80^\circ C$ until the solution became highly viscous to obtain the branched SPI with high molecular weight [11]. The *m*-cresol solutions of SPIs were cast onto glass plates and dried at

120 °C for 10 h. The as-cast membranes were immersed in methanol at 60 °C for 1 h and then proton-exchanged with 0.25 mol/L H₂SO₄. After being washed with water, the membranes were dried at 150 °C for 10 h in vacuo. The membrane thickness was 20–60 μm.

Proton conductivity σ in plane direction of membrane was measured using a four-point-probe electrochemical impedance spectroscopy technique with a LCR meter (HIOKI 3532-80).

Pt/C fuel electrodes (Vulcan XC-72, E-TEK Inc., Pt load: 0.5 mg/cm²) were impregnated with 1.5 mg/cm² of Nafion by applying 0.036 ml/cm² of 5 % Nafion (EW: 1100) solution to retain better contact with the membrane. A membrane electrode assembly (MEAs) was prepared by hot-pressing the electrodes onto a membrane at 135 °C for 10 min under 80 kg/cm². The MEA was installed in a single-cell (E-TEK, active area: 5 cm²), which was then set in a fuel cell test system (nF Inc., model As-510). PEMFC experiments were carried out at a cell temperature of 70 °C and humidifier temperatures of 70 and 68 °C for anode and cathode, respectively, using H₂ and O₂ with a feed rate of 200 ml/min and a total pressure of 0.3 MPa, unless otherwise noted.

3. RESULTS AND DISCUSSION

3.1 Proton conductivity of SPIs

The relative humidity (RH) dependence of proton conductivity of SPIs and Nafion115 at 50 °C is shown in Fig.2. With an increase in RH, the conductivity increased much more largely for SPIs than for Nafion 115. Although the conductivities of SPIs were much smaller than those of Nafion 115 at lower RHs, at higher RHs above 90 %RH the conductivities of SPIs are comparable to or slightly larger than those of Nafion 115 ($\sigma > 0.1$ S/cm). The linear and main-chain type of SPI, NTDA-BAPBDS/BAPB(2/1), showed slightly smaller

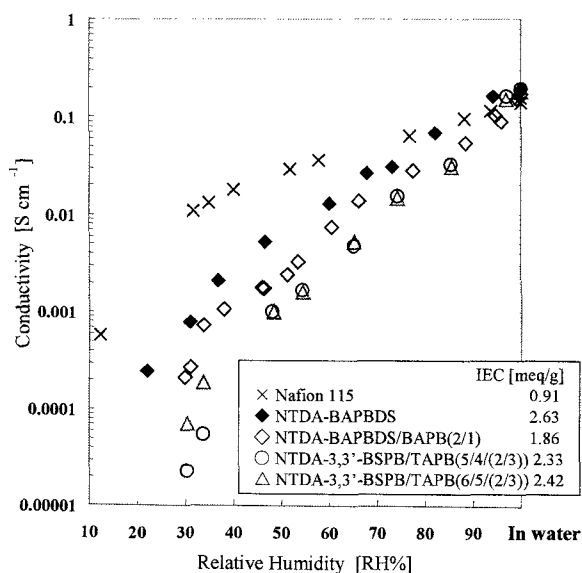


Fig.2 Relative humidity dependence of proton conductivity for SPI membranes at 50 °C.

conductivity in the whole RH range than the corresponding homopolymer, NTDA-BAPBDS, because of the lower ion exchange capacity (IEC) and smaller water uptake. The branched, crosslinked and side-chain type of SPIs, NTDA-3,3'-BSPB/TAPB (6/5/(2/3)) and (5/4/(2/3)), showed the slightly larger RH dependence of conductivity than the linear and main-chain type SPIs. The former displayed high proton conductivities close to or slightly higher than those of the latter ones in the high RH range above 90 RH%, but much lower conductivities in the lower RH range.

3.2 Fuel cell performance

3.2.1 Linear and main-chain type of SPI

Figure 3 shows the fuel cell performance of MEAs based on Nafion 115 (125 μm in thickness) and NTDA-BAPBDS/BAPB(2/1) (55 μm). The open circuit voltage (OCV) was about 0.97 V for Nafion 115 and 0.94 V for the SPI.

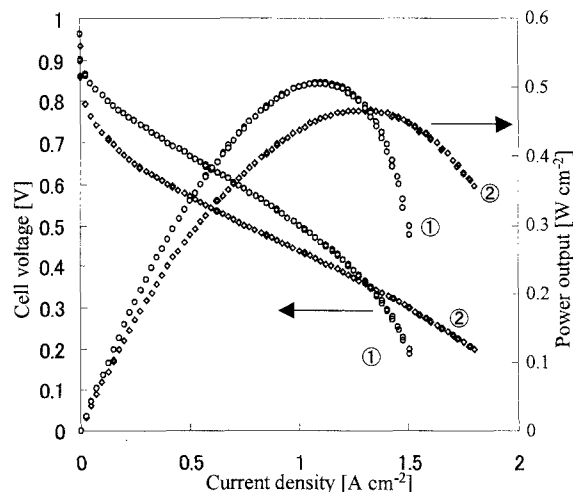


Fig.3 Cell performance of MEAs with Nafion 115 (①) and NTDA-BAPBDS/BAPB(2/1) (②).

The present MEA of Nafion 115 showed a cell voltage (V) of 0.50V at a current density (I) of 1 A/cm², which was somewhat lower than 0.55 V for Nafion 115 reported by Besse et al. [12]. Taking the higher feed pressure (0.4 MPa) for the latter into account, these MEAs of Nafion 115 are considered to have the similar cell performance. They also reported the I - V curves for MEAs of SPIs derived from NTDA, 2,2'-benzidinedisulfonic acid (BDSA) and nonsulfonated diamines. Their MEAs of the BDSA-based SPIs showed much lower cell performance than their MEA of Nafion115, that is, the cell voltages of 0.40 and 0.20 V at 1 A/cm² for the SPIs with IECs of 1.98 and 1.26 meq/g, respectively [12]. The MEA of NTDA-BAPBDS/BAPB (2/1) showed the cell voltage of 0.45 V at 1 A/cm², which was lower than that of Nafion 115 but higher than that of the BDSA-based SPIs mentioned above. The maximum output was 0.48 W/cm² at 1.3 A/cm² for NTDA-BAPBDS/BAPB(2/1) and 0.51 W/cm² at 1.1 A/cm² for Nafion 115.

3.2.2 Branched, crosslinked and side-chain type of SPIs

Figure 4 shows the cell performance of MEAs of NTDA-3,3'-BSPB/TAPB (6/5/(2/3)) and (5/4/(2/3)) of 35 and 25 μm , respectively, in thickness. The OCV was 0.96 V, which was similar to that of Nafion 115. The maximum outputs were 0.84 and 1.26 W/cm^2 at 2.1 and 3.7 A/cm^2 for NTDA-3,3'-BSPB/TAPB (6/5/(2/3)) and (5/4/(2/3)), respectively, which were 1.6 and 2.5 times larger than those of Nafion 115 and NTDA-BAPBDS/BAPB(2/1). The lower performance of Nafion 115 is attributed mainly to the much larger membrane thickness. Recently, we prepared a MEA with Nafion 112 of 55 μm in thickness and confirmed its high performance of a maximum output of 0.80 W/cm^2 at 2.1 A/cm^2 under the same operation conditions [13].

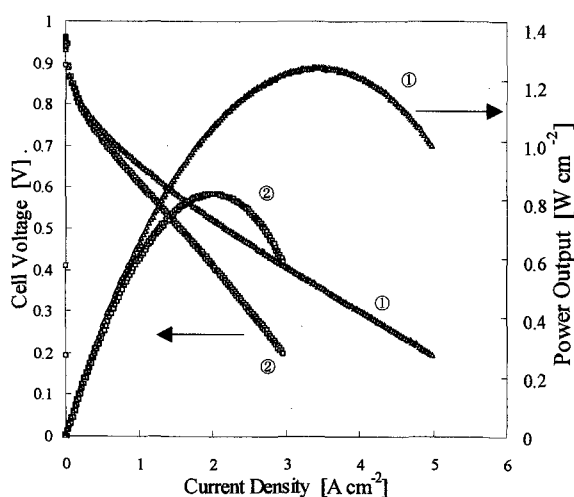


Fig.4 Cell performance of MEAs with NTDA-3,3'-BSPB/TAPB(5/4(2/3)) (①) and NTDA-3,3'-BSPB/TAPB(6/5(2/3)) (②).

As mentioned above in Fig. 2, in the high RH range above 90 %RH, Nafion 115 and the two types of SPIs investigated here had high proton conductivities of 0.1 S/cm or more and the difference in conductivity was

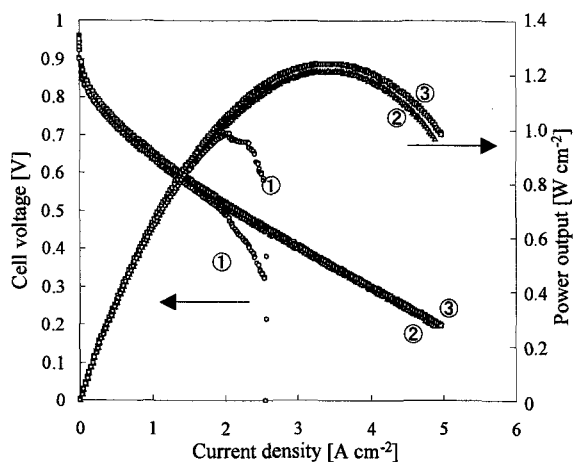


Fig.5 Effects of flow gas rate for cell performance of MEA with NTDA-3,3'-BSPB/TAPB (5/4(2/3)). Gas flow rate:① 50, ② 100 and ③ 200 ml/min.

rather small. This suggests that in the fully hydrated state the membrane thickness would not have such significant effects on the I - V characteristics. Therefore, it is reasonable to consider that the proton conductivity of membrane in MEA was much lower than that estimated from Fig. 2. The probable reasons are the difference in proton flow direction (the protons move in thickness direction of membrane in the case of MEA, but in plane direction in the case of conductivity measurement) and any difference in the hydrated state of the membrane (the membrane in MEA might not be fully hydrated). The much better cell performance of MEAs of NTDA-3,3'-BSPB/TAPB (6/5/(2/3)) and (5/4/(2/3)), compared with NTDA-BAPBDS/BAPB (2/1), seemed due to better contact of membrane and Pt/C electrodes as well as the smaller membrane thickness. Further study is necessary to achieve superior MEA fabrication.

3.2.3 Effects of operating conditions on cell performance

As shown in Fig. 5, the gas flow rate hardly affected the cell performance unless the fuel gas ran short.

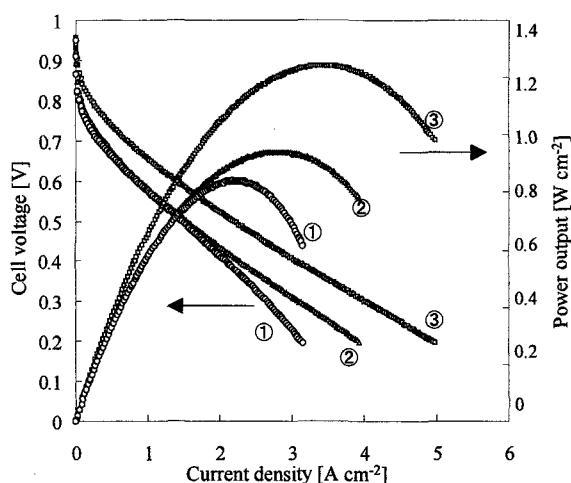


Fig.6 Effects of gas pressure for cell performance of MEA with NTDA-3,3'-BSPB/TAPB (5/4(2/3)). Gas pressure : ① 0.1, ② 0.2 and ③ 0.3 MPa.

Figure 6 shows effect of gas feed pressure on the cell performance for the MEA of NTDA-3,3'-BSPB/TAPB (5/4/(2/3)). With increasing the feed gas pressure up to 0.3 MPa, the potential drop in the range of the low current density became smaller due to better gas diffusion in the three-phase interface, resulting in the significant improvement of the cell performance.

Figure 7 shows effect of cathode gas, oxygen or air, on the cell performance for the MEA of NTDA-3,3'-BSPB/TAPB (5/4/(2/3)). When air gas consisting of 79 % N_2 and 21 % O_2 was supplied at a flow rate of 1000 ml/min in stead of pure oxygen, the I vs. V curve hardly changed in the range of low current density below 0.5 A/cm^2 , but in the range above it the cell voltage decreased largely with increasing the current density, resulting in a much lower maximum output of 0.58 W/cm^2 at 1.2 A/cm^2 . The similar reduction (50 %) of the maximum output was also reported for the MEA of Nafion [14].

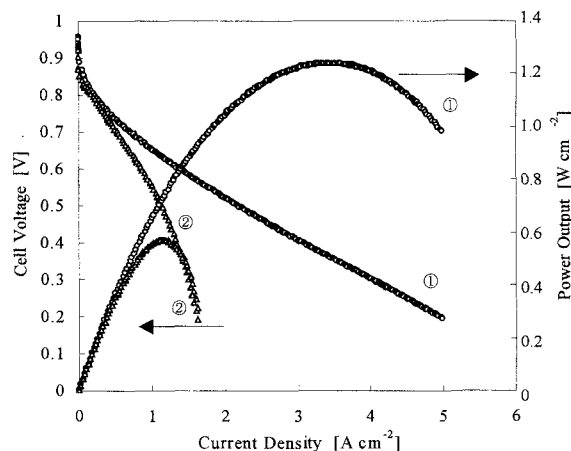


Fig.7 Cell performance of MEAs with NTDA-3,3'-BSPB/TAPB (5/4(2/3)). Feed gas : ① H₂/O₂ and ② H₂/air.

4. CONCLUSIONS

MEAs made from the branched, crosslinked and side-chain type of SPIs, especially NTDA-3,3'-BSPB/TAPB(5/4(2/3)), showed the excellent cell performance of maximum output of 1.26 W/cm² at 3.7 A/cm². On the other hand, MEAs made from the linear main-chain type of SPI displayed much poorer performance probably because of the poor contact of membrane and electrode interface. Further study is necessary to achieve superior MEA fabrication.

5. REFERENCES

- [1] O. Savadogo, *J. New Mater. Electrochem Systems*, **1**,47 (1998)
- [2] V. Mehta and J. S. Cooper, *J. Power Sources*, **114**, 32 (2003).
- [3] C. Genies, R. Mercier, B. Sillion, N. Cornet, G. Gebel and M. Pineri, *Polymer*, **42**, 359 (2001). *Polymer*, **42** 359 (2001).
- [4] N. Cornet, O. Diat, G. Gebel, F. Jousse, D. Marsacq, R. Mercier and M. Pineri. *J. New. Mat. Electrochem. Systems*, **3**, 33 (2002).
- [5] J. Fang, X. Guo, T. Watari, K. Tanaka, H. Kita and K. Okamoto, *Macromolecules*, **35** 6707 and 9022 (2002).
- [6] K. Okamoto, *J. Photopolym. Sci. Technol.*, **16** 247 (2003).
- [7] T. Watari, J. Fang, X. Guo, K. Tanaka, H. Kita, K. Okamoto and K. Hirano, *Kagakukougaku Ronbunshu*, **29**, 165 (2003).
- [8] T. Watari, J. Fang, K. Tanaka, H. Kita, K. Okamoto and T. Hirano, *J. Membr. Sci.*, in press.
- [9] Y. Yin, J. Fang, H. Kita and K. Okamoto, *Chem. Letters*, **32**, 328 (2003).
- [10] Y. Yin, J. Fang, H. Kita and K. Okamoto, submitted to *J. Mater. Chem.*
- [11] S. Hayashi, Y. Yin, Y. Sudo, K. Tanaka, H. Kita and K. Okamoto, *Polym. Prep. Jpn.*, **52**, 3494 (2003).
- [12] S. Besse, P. Capron, O. Diat, G. Gebel., F. Jousse, D. Marsacq, M. Pineri, C. Marestin and R. Mercier, *J. New. Mat. Electrochem. Systems*, **5** 109 (2002)
- [13] O. Yamada, Y. Yin, K. Tanaka, H. Kita and K. Okamoto, *The 44th Battery Symposium in Japan*, 148 (2003).

[14] J. N. Han, G. Park, Y. Yoon, T. Yang, W. Lee and C. Kim, *International J. Hydrogen Energy*, **28** 609 (2003).

(Received October 13, 2003; Accepted March 16, 2004)